

SUPPLEMENTARY INFORMATION

Boosting nanotoxicity to combat multidrug-resistant bacteria in pathophysiological environments

5 Dana Westmeier^{1, #}, Svenja Siemer^{1, #}, Cecilia Vallet², Jörg Steinmann³, Dominic Docter¹, Jan Buer³, Shirley K. Knauer^{2, *} and Roland H. Stauber^{1, 4*}

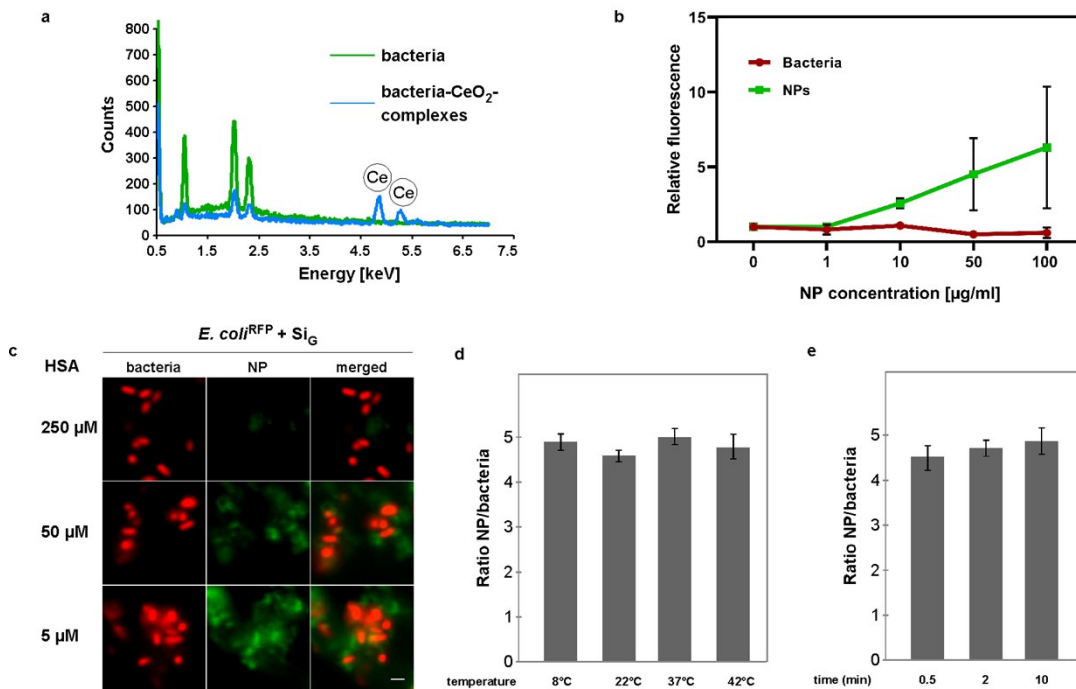
Table of Contents

SUPPLEMENTARY FIGURES		<i>page</i>
10	S1 Characterization of NM-pathogen assembly <i>in situ</i> .	S2
	S2 NM-bacteria complex formation mediates antibacterial effect.	S3
	S3 NM-bacteria complex formation is enhanced by low pH conditions.	S4
	S4 The <i>Galleria mellonella</i> larvae skin infection model.	S5
15	SUPPLEMENTARY TABLES	
	S1 Colloidal stability of NMs in different media.	S6
	S2 List of plasma corona proteins identified by LC-MS for Ag and CuNMs	S7
	S3 Composition of the simulated wound fluid (SWF).	S8

20

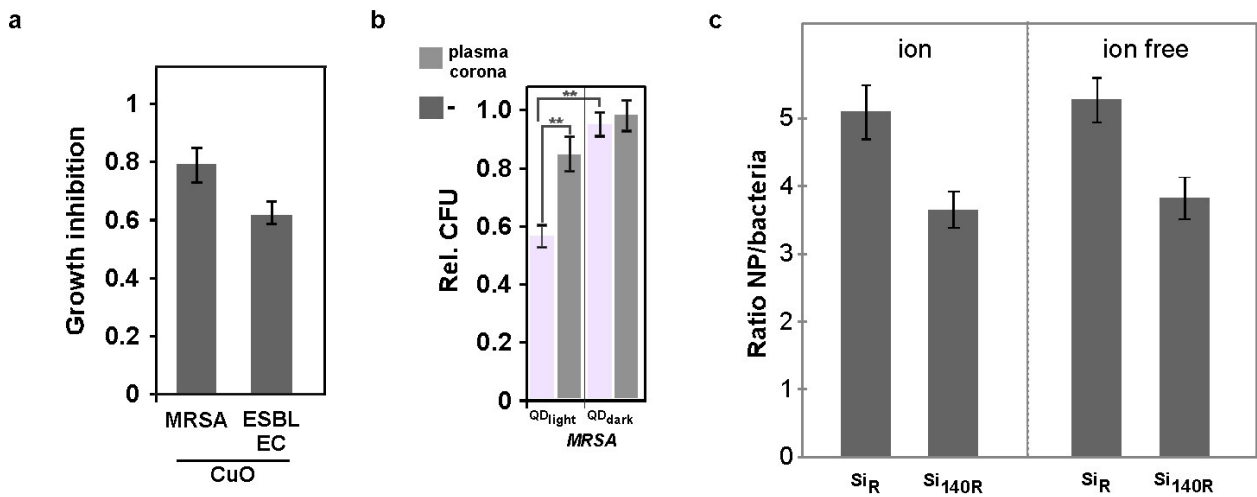
SUPPLEMENTARY FIGURES

Supplementary Fig. S1



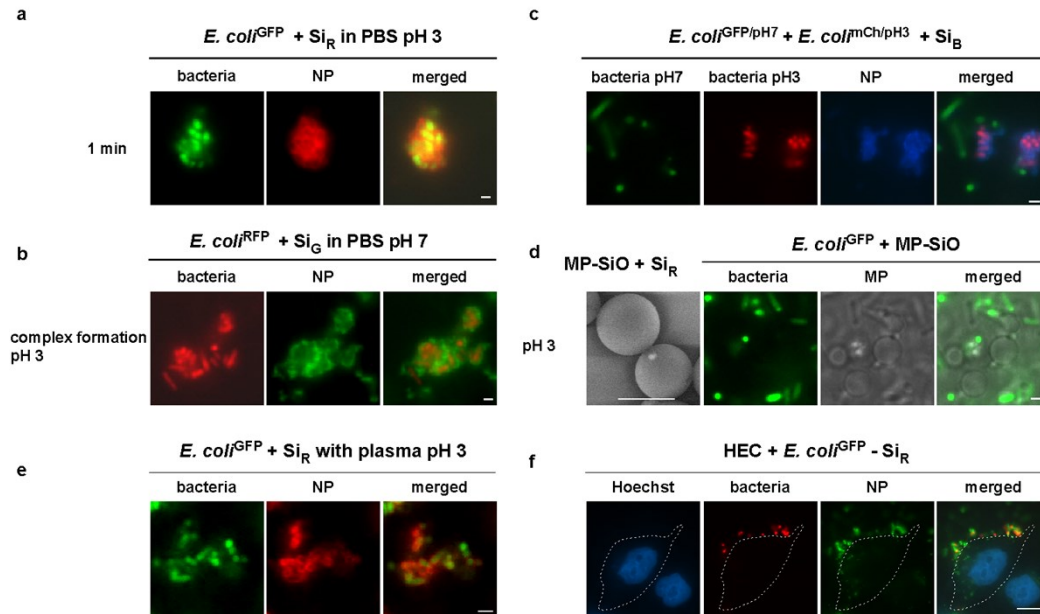
- 5 **Supplementary Figure S1| Characterization of NM-pathogen assembly *in situ*.** **a**, EDX shows a distinct peak for cerium for bacteria pre-incubated with CeO₂-NMs according to the SOP which is absent in the control. **b**, Increasing amount of NMs results in higher numbers of NM-bacteria complexes *in situ*. Quantification using automated high-throughput microscopy employing the *TargetActivation* assay. **c**, Human serum albumin (HSA) concentration dependently decreases
- 10 NM-bacteria complex formation for red fluorescent *E.coli* bacteria pre-incubated with green-fluorescent silica NMs. Fluorescent microscopy of unfixed samples. Scale bar, 2 µm. **d**, The temperature during pre-incubation of bacteria with NMs (5 min) does not influence complex formation in a range from 8-42 °C. Quantification using automated high-throughput microscopy employing the *TargetActivation* assay. **e**, Bacteria-NM complex formation is a quick process (<30s)
- 15 with no apparent increase in ratio of NMs/bacteria from 30s onwards. Quantification using automated high-throughput microscopy employing the *TargetActivation* assay.

Supplementary Fig. S2



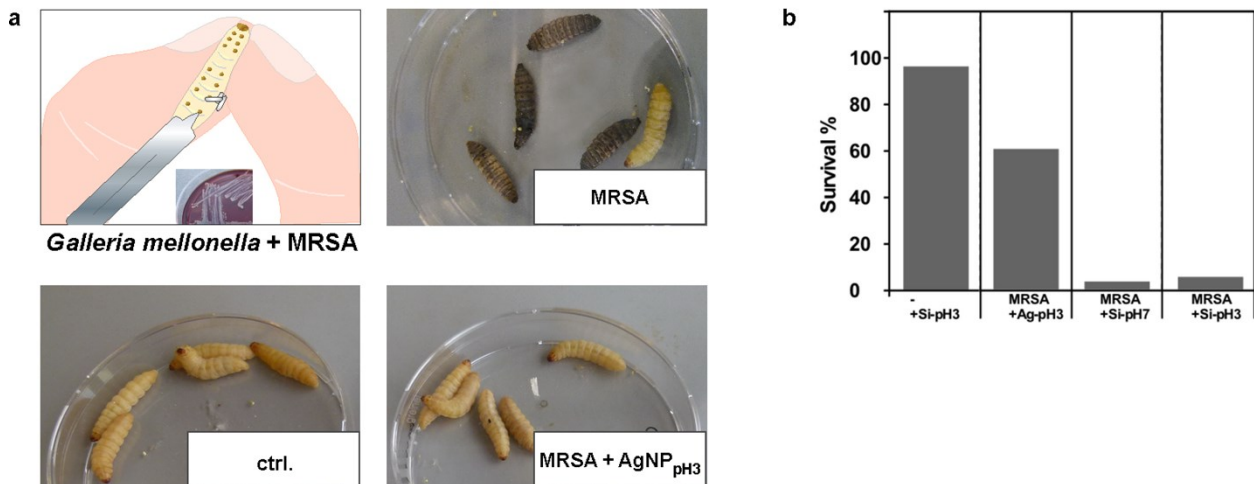
Supplementary Figure S2| NM-bacteria complex formation mediates antibacterial effect. a, Improved killing of G⁺ (MRSA) over G⁻ (ESBL EC) pathogens by CuO NMs (50 µg/mL). **b,** Quantum dot-mediated antibacterial activity is independent of NM dissolution but dependent on corona-formation. **c,** Improved binding of small Si NM (∅~30 nm versus ∅~140 nm) is independent of counter ions. Incubation was performed in PBS (ion) or desalted water (ion-free) conditions. **a-c,** Quantification was performed using automated high-throughput microscopy employing the *TargetActivation* assay. Data are representatives of two independent experiments.

Supplementary Fig. S3



Supplementary Figure S3| NM-bacteria complex formation is enhanced by low pH conditions. **a**, NM-bacteria complex formation was enhanced after short (1 min) acidic exposure of NMs and bacteria in PBS. Scale bar, 2 μm. **b**, NM-bacteria complexes formed under acidic conditions (pH 3) remained intact when subsequently incubated under neutral conditions (pH 7). Scale bar, 2 μm. **c**, Bacteria, pre-treated at pH 3, and bacteria, pre-treated at pH 7, were mixed with NMs at neutral conditions (pH 7). NMs preferentially assembled on pH 3-treated pathogens. **d**, Si_R NMs and bacteria did not bind to microparticles (MP-Si), even under acidic conditions (pH 3). Scale bar, 2 μm. **e**, Bacteria and Si_R NMs form complexes under acidic conditions even with plasma present. Scale bar, 2 μm. **f**, NM-bacteria complexes attach to human epithelial cells (HEC) and remain stable after incubation of 90 min. Cells were washed, fixed and the nucleus stained (Hoechst). Scale bar, 10 μm.

Supplementary Fig. S4



Supplementary Figure S4| The *Galleria mellonella* larvae skin infection model. **a**, The relatively large size of *Galleria mellonella* larvae allows the controlled skin infection with pathogens and testing of the therapeutical and/or toxicological activity of NMs. *Galleria mellonella* larvae are an easy to handle, low cost *in vivo* model for (pre-)screening of NMs and ethically less problematic compared to vertebrate models. Survival p.i. can be recorded by visual inspection (high level of skin melanisation and hardening) and testing signs of vitality by brief touching. Compared to controls, infection with MRSA leads to animal death, which could be prevented by application of pH 3 AgNMs. Representative animals from the experiment shown in Fig. 4a are displayed.

b, To further exclude pH effects in the wound microenvironment, such as fibroblast proliferation or macrophage activity, we additionally controlled the impact of pH on bacterial infection by employing our *Galleria in vivo* model (Supplementary Fig. S)

Galleria mellonella larvae were scratched with a lancet, and 5 μ L of Gram-positive Methicillin-resistant *Staphylococcus aureus* (MRSA) (4.0×10^7 CFU/mL) used to infect the wound. Subsequently, 5 μ L of AgNMs pH3 (AgNMs: 0.1 mg/mL; 1% PEG₆₀₀, 1 mM citrate), 5 μ L of Si₃₀ NMs pH 3 (Si₃₀ NMs: 1 mg/mL; 1% PEG₆₀₀, 1 mM citrate) or 5 μ L of Si₃₀ NMs pH 7 (Si₃₀ NMs: 1 mg/mL; 1% PEG₆₀₀, PBS) formulations were used. Control: 5 μ L of Si₃₀ NMs pH 3 (Si₃₀ NMs: 1 mg/mL; 1% PEG₆₀₀, 1 mM citrate) without MRSA infection. Animal death was monitored 6 day p.i. The % of dead animals is indicated (n=30 for each group). Results of a representative experiment is shown. In contrast to pH 3 AgNMs, the applications of Si₃₀ NMs at pH 3 or pH 7 did not prevent bacterial growth and animal death, excluding a significant bacteriocidal effect of low pH without antibiotic NMs.

SUPPLEMENTARY TABLES

Supplementary Table S1 | Colloidal stability of NMs in different media.

Nanomaterial	TEM	DLS		Zeta potential	
	Diameter	Hydrodynamic diameter		± SD [mV]	
	± SD [nm] in dry state	± SD [nm], (PDI) in buffer-A	plasma*	in buffer-A	plasma*
Si₃₀	31.4 ± 5.8	33 ± 7	48 ± 3	-15 ± 2	-14 ± 2
Ag	10.3 ± 2.2	11.4 ± 3	32 ± 7	-43 ± 1	-41 ± 3

Supplementary Table S1. Colloidal stability of NMs in different media. The average size of the different nanomaterials was determined in dry state (TEM) as well as in buffer-A by DLS. Plasma measurements were performed 10 min post exposure to plasma (plasma*), followed by plasma separation and subsequent washing. Zeta potentials were determined with a Zetasizer. Values are mean ± SD from three independent experiments. Polydispersity index (PDI) was calculated as the square of the standard deviation over diameter.

Supplementary Table S2. List of plasma corona proteins identified by LC-MS for Ag and CuNMs. Exposure time: 15 min. Calculated isoelectric point, molecular weight, functional annotation, intracellular localization as well as their relative abundance calculated from three
5 technical replicates. Complete and summarized datasets are given in supporting information file: Westmeier_Suppl_Table_S2.xlsx.

Supplementary Table S3 | Simulated wound fluid (SWF)

Components	SWF
Sodium chloride	5.844 g/L
Sodium hydrogen carbonate	3.360 g/L
Potassium chloride	0.298 g/L
Calcium chloride	0.277 g/L
Human serum albumin	33 g/L
Hydrochloric acid	for SWF pH 3

Supplementary Table S3. Composition of the simulated wound fluid (SWF).